J. Biochem. 124, 79-88 (1998)

Molecular Cloning, Expression, and Site-Directed Mutagenesis of Inorganic Pyrophosphatase from *Thermus thermophilus* HB8[1]

Takanori Satoh,* Tatsuya Samejima,*,[2] Machiko Watanabe,* Shin-ichi Nogi,* Yoshimasa Takahashi,* Hiroyuki Kaji,*,[3] Alexei Teplyakov,† Galya Obmolova,† Inna Kuranova,‡ and Keisuke Ishii*,[4]

*Department of Chemistry, College of Science and Engineering, Aoyama Gakuin University, Chitosedai, Setagaya-ku, Tokyo 157-8572; †European Molecular Biology Laboratory, c/o DESY, Notkestr. 85, 22603 Hamburg, Germany; and ‡Institute of Crystallography, Leninsky pr. 59, Moscow 117333, Russia

Received for publication, January 27, 1998

The genomic DNA encoding the inorganic pyrophosphatase from an extremely thermophilic bacterium, *Thermus thermophilus* HB8 (ATCC27634), was isolated by colony hybridization with a probe designed as a part of gene amplified by the PCR method, which was derived from the partial amino acid sequence of the enzyme. The DNA was cloned into a plasmid vector, pUC118, after digestion with *Bam*HI. The inserted nucleotide fragment was about 1.8 kbp in length and the nucleotide sequence included a 525 bp open reading frame. The deduced amino acid sequence was completely identical with that of the enzyme determined by automated Edman analysis of peptide fragments isolated from digests obtained with *Staphylococcus aureus* V8 protease and *Achromobacter* protease I, and also from products obtained on chemical cleavage with cyanogen bromide and 70% formic acid. The subunit of this enzyme is composed of 174 amino acid residues with a calculated molecular weight of 19,084. Then, the gene was overexpressed in *Escherichia coli* BL21 (DE3) using a plasmid vector, pET15b, system. The recombinant enzyme was fully active, and exhibited higher thermostability than the *E. coli* enzyme. Amino acid residues located on the surface of the recombinant enzyme were determined by means of limited proteolysis, and the results revealed that the environment of Lys residues is almost the same as the crystal structure reported previously [Teplyakov, A. *et al.* (1994) *Protein Sci.* 3, 1098-1107]. Furthermore, the roles of two tryptophan residues were investigated by site-directed mutagenesis, which indicated that they may be responsible for the structural integrity and thermostability.

Key words: amino acid sequence, inorganic pyrophosphatase, molecular cloning, site-directed mutagenesis, *Thermus thermophilus*.

Inorganic pyrophosphatase (PPase [EC 3.6.1.1]) catalyzes the hydrolysis of inorganic pyrophosphate to two orthophosphate molecules, and plays an important role in providing a thermodynamic driving force for many biosynthetic reactions in cells (*1*). PPase is ubiquitously present in the cytosol of organisms from vertebrates to microbes, and has been isolated from various sources and characterized. The best studied PPases are those from *Saccharomyces cerevisiae* (Y-PPase) and *Escherichia coli* (*E. coli* PPase), which commonly require divalent cations, being most effective, Mg^{2+} for their activity and stability, although they have different subunit structures (*2*). Procaryotic PPases consist of six identical subunits with molecular weights of *ca.* 18-20 kDa, whereas eucaryotic PPases are homodimers of 30-35 kDa subunits. Extensive studies on chemical modification and site-directed mutagenesis of these PPases have indicated that several amino acid residues may be essential for catalytic activity and substrate binding (*3-5*). The genes for bacterial PPases have been cloned and their amino acid sequences were deduced from their base sequences (*6, 7*). Recently, the amino acid sequence of PPase from thermophilic bacterium PS-3 was directly determined by automatic Edman degradation (*8*) and also genomic cloning (*9*). Meanwhile, we have determined the amino acid sequence of the PPase from *Bacillus stearothermophilus* (*Bst* PPase) by both Edman degradation and deduction from the base sequence of the gene

[1] This study was partly aided by a grant from the Research Institute of Aoyama Gakuin University. The nucleotide sequence reported in this paper has been submitted to the DDBJ, Gen Bank, and EMBL nucleotide databases under accession number, AB010580. The amino acid sequence reported in this paper has been submitted to the SWISS-PROT protein sequence database under accession number, P38576.

[2] To whom correspondence should be addressed. Tel: +81-3-5384-1111 (Ext. 3204), Fax: +81-3-5384-6200, E-mail: samejima@candy.chem.aoyama.ac.jp

Present addresses: [3] Department of Chemistry, Faculty of Science, Tokyo Metropolitan University, Minami-osawa, Hachioji, Tokyo 192-0364; and [4] Department of Development, Shino-Test Co., Oonodai, Sagamihara, Kanagawa 229-0011.

Abbreviations: PPase, inorganic pyrophosphatase; *Tth*, *Thermus thermophilus*; Y, *Saccharomyces cerevisiae*; *Bst*, *Bacillus stearothermophilus*; API, *Achromobacter* protease I.

(unpublished result). The results of alignment of the amino acid sequences of these PPases suggested that the amino acid residues participating in the catalytic activity are almost all conserved. Furthermore, recent analysis of the three-dimensional X-ray crystallographic structures of Y-PPase, *E. coli* PPase, and the PPase from *Thermus thermophilus* (*Tth*) HB8 provided important information on the catalytic mechanisms involving Mg^{2+} and the substrate binding sites (*10-13*). With respect to thermostability, it was suggested that some interactions and oligomerization contribute to the thermostability of *Tth* PPase (*14*). In this paper, we report the entire amino acid sequence of PPase from *Tth*, having an optimal growth temperature of 80°C, and the base sequence of the cloned *Tth* PPase gene. Also, several candidate amino acids contributing to the thermostability were deduced on comparison of the amino acid sequence of *Tth* PPase with those of procaryotic PPases, and also from the results of studies involving limited proteolysis and site-directed mutagenesis.

MATERIALS AND METHODS

Protein Sequencing—Soluble inorganic pyrophosphatase from *Tth* HB8 was isolated and purified as described (*15*). It was first reduced and pyridylethylated by the method of Friedman *et al.* (*16*). Enzymatic cleavage of the *S*-pyridylethylated protein with *S. aureus* V8 protease (Worthington) and API (Wako Pure Chemicals) was carried out at 37°C for 12 and 6 h, respectively, after denaturation with 4 M urea. Chemical cleavage between the Asp and Pro residues of the *S*-pyridylethylated protein was performed in 70% formic acid at 37°C for 48 h. Chemical scission with cyanogen bromide (Wako Pure Chemicals) was also carried out in 70% formic acid at 4°C for 24 h. The peptides were separated by reverse phase HPLC on a Biofine RPC-SC18 column (JASCO) with a linear gradient of 0-80% acetonitril in 0.1% TFA. The isolated peptides were sequenced by automatic Edman degradation using a PSQ-1 automatic gas-phase protein sequencer (Shimadzu).

Bacterial Strains—*E. coli* JM109 was grown in a Luria-Bertani (LB) medium at 37°C and transformed by the method of Chung *et al.* (*17*). *Tth* HB8 was grown in 350 ml of a medium comprising 0.8% polypeptone, 0.4% yeast extract, and 0.3% NaCl at 65°C (*18*).

Genomic DNA Preparation—Genomic DNA of *Tth* HB8 was extracted as follows, *i.e.* essentially according to the method of Maniatis *et al.* (*19*). A frozen cell pellet was suspended in 10 ml of 100 mM Tris-HCl (pH 7.6)-150 mM EDTA-150 mM NaCl, and then lysed with lysozyme (1 mg/ml, 1 h, 37°C) and 1% SDS (15 min, 60°C). The lysate was treated with proteinase K (1 mg/ml, 8 h, 50°C) and RNase A (1 mg/ml, 1 h, 37°C), and then extracted three times with phenol. Finally, the DNA was collected by ethanol precipitation.

Oligonucleotide Primers—Degenerate oligonucleotide primers encoding the internal sequence of *Tth* PPase were prepared by chemical synthesis. These primers had the sequences 5′-AAYAARTAYGARTAYGAYCC-3′ (20mer, corresponding to amino acid residues 28-34) and 5′-GTY-TCRAARAARTGYTG-3′ (17mer, corresponding to 133-138), respectively, where Y denotes T or C, and R denotes A or G. PCR amplification was achieved by incubating a mixture comprising 100 ng of genomic DNA, 20 pmol of each primer, 1 mM of each dNTP and 2.5 units of *Taq* DNA polymerase at 92°C for 1 min, followed by 30 reaction cycles with a temperature program of 92°C for 1 min, 35°C for 1 min, and 72°C for 2 min. The PCR product was treated with Klenow fragment. The obtained 333-bp PCR product was used as a probe.

Screening of a Genomic Library—The obtained genomic DNA mixture was fragmented with *Bam*HI and then separated on a 1.5% agarose gel, followed by isolation of DNA fragments of about 1.8 kbp in length. The fragments were cloned into the *Bam*HI site of a plasmid vector, pUC118. Screening for the gene encoding the PPase from *Tth* HB8 was carried out by colony hybridization. For colony hybridization, colonies of *E. coli* JM109 transformed with this plasmid were transferred to a nitrocellulose membrane filter, lysed in 1% SDS and 5 mM EDTA, and then UV crosslinked and hybridized in a formamide-based solution for 6 h at 42°C with the 333-bp PCR product as a probe by the method for the DIG Luminescence Detection Kit (Boehringer Mannheim). The filter was washed twice at room temperature in a 2×SSC and 1% SDS solution, and then exposed to X-ray film for 30 min.

Nucleotide Sequencing—The base sequence was determined by the dideoxy chain termination method with *Bca* BEST polymerase (TAKARA) using a DNA sequencer model SQ-3000 (Hitachi).

Construction of an Expression Vector for Tth PPase—An expression vector for *Tth* PPase, pETTP, was constructed as follows. At first, we constructed a plasmid vector, pUCTP, in which the *Tth* PPase gene was cloned as described above. The pUCTP vector was used as the template for PCR in order to construct the expression vector. The sense-primer for add-on PCR corresponding to Ala-1-Leu-3 with initiation codon ATG, was 5′-GGGAAT-TCCATGGCGAACCTG-3′ (21mer). The antisense-primer to Arg-171-Gly-174 with stop codon TAG was 5′-AAGGA-TCCTTAGCCCTTGTAGC-3′ (22mer). The once amplified DNA fragment was inserted into the *Eco*RI-*Bam*HI site of a plasmid vector, pUC118, and then sequenced. Thus, we constructed a pUCTPPCR vector. After digestion with *Nco*I and *Bam*HI endonucleases, the fragment was inserted into the *Nco*I-*Bam*HI site of the pET15b vector (TAKARA), yielding the expression vector named pETTP.

Site-Directed Mutagenesis by Polymerase Chain Reaction—Site-directed mutagenesis was performed by means of polymerase chain reaction. Two variants, W149F and W149F-W155F, were constructed as described below. The sense-primer for W149F was 5′-GGCTCGAGGCTAAGA-AGGGGAAGTTTGTCAAG-3′ (32mer, corresponding to Leu-142-Lys-151). The antisense-primer for W149F was 5′-CGCGGAGACGTCAGAGCTTGT-3′ (22mer, which was complementary to a sequence in the pUC118 vector). The amplified fragment was digested with *Xho*I and *Nae*I, and then inserted into pUCTPPCR after digestion with the same endonucleases. Then, it was sequenced, digested with *Nco*I and *Bam*HI, and then inserted into the same site of the pET15b vector, the resultant variant being named pTPW149F. The other variant, W149F-W155F, was constructed by means of the recombinant PCR method (*20*). The pTPW149F vector was used as the template for PCR. The upper fragment was amplified by using a sense-primer, 5′-GGGAATTCCATGGCGAACCTG-3′ (21mer, the same

primer as described above), and an antisense-primer, 5′-CCTTCCGGTCCCGAAAGCCCGTGAC-3′ (25mer, corresponding to Val-152-Lys-159). Meanwhile, the lower fragment was amplified with a sense-primer, 5′-GGGCTTTCGGGACCGGAAGGCGGCTCTAGAGGA-3′ (33mer, corresponding to Gly-154-Lys-159), and an antisense-primer, 5′-CGCGGAGACGTCAGAGCTTGT-3′ (22mer, the same primer as described above). The upper and lower fragments amplified in the first PCR were denatured and annealed, followed by the second PCR. The amplified DNA fragment was digested with *Xho*I and *Bam*HI, and then inserted into the same site of the pUCTPPCR vector. Then, it was sequenced, digested with *Nco*I and *Bam*HI, and then inserted into the same site of the pET15b vector.

Purification of the Recombinant Tth PPase—Purification of the recombinant *Tth* PPase was performed as follows. *E. coli* BL21 (DE3) cells transformed with the expression vector, pETTP, were cultured in 1 liter of LB/Amp medium at 37°C for 20 h. The cells were harvested by centrifugation and then lysed by sonication, the soluble fraction being collected. This fraction was subjected to DEAE-Sephacel (Pharmacia) anion-exchange column chromatography, followed by Sephacryl S-200HR (Pharmacia) gel filtration chromatography. If necessary, HPLC on an anion-exchange column was performed until the enzyme gave a single band on polyacrylamide gel electrophoresis.

Enzyme Assay—The activity of PPase was assayed at 37°C essentially according to the method described previously (*21*), the liberation of inorganic phosphate being determined by the method of Peel and Loughman (*22*). Protein concentrations were determined by the method of Lowry *et al.* (*23*), using bovine serum albumin as the standard.

SDS-Polyacrylamide Gel Electrophoresis (SDS-PAGE)—SDS-polyacrylamide gel electrophoresis was performed by the method of Laemmli (*24*), on a 15% polyacrylamide gel. The proteins were stained with Coomassie Brilliant Blue R-250.

Circular Dichroism (CD) Spectra Measurements—CD spectra were recorded with a J-600 automatic recording dichrograph (JASCO) at room temperature with protein concentration of 0.1-0.2 mg/ml. Far-UV CD spectra were measured, between 200 and 250 nm, in a 1 mm optical path cuvette. CD data are expressed in terms of mean residue ellipticity, $[\theta]$, using the mean residue molecular weight determined from the determined primary structure.

Fluorescence Measurements—Fluorescence measurements were made with an FP777 spectrofluorometer (JASCO) at room temperature. The protein concentration was always adjusted to 0.1 mg/ml with 20 mM Tris-HCl buffer (pH 7.8). Tryptophan excitation was at 295 nm, whereas tyrosine excitation was at 275 nm. Both emission spectra were set between 300 and 400 nm.

Limited Proteolysis through Digestion with API—Limited proteolysis of the recombinant *Tth* PPase was performed as described below: the purified recombinant *Tth* PPase was dialyzed against 50 mM Tris-HCl buffer (pH

```
-180 CCGGGATCGGCGAGCTCCAGGCGTTGCACCCCCTGGTCGCTCAGGAAGAGGAGCGCCGTT

-120 TCCGTGACCGCGAGAAGCCCCTCCGGCCCTCCAGTTGGGCGAGGGGGCGCTCCCCGAGAC

 -60 GGGCGAGCTCGGCTTCATACTTGCCCATGGCCCCATTCTATACGGCATAATGGGggcggT

   1 ATGGCGAACCTGAAGAGCCTTCCCGTGGGCGACAAGGCGCCCGAGGTGGTCCACATGGTC
   1 M  A  N  L  K  S  L  P  V  G  D  K  A  P  E  V  V  H  M  V

  61 ATTGAGGTCCCCCGCGGCTCGGGCAACAAGTACGAGTACGACCCGGACCTCGGGGCGATC
  21 I  E  V  P  R  G  S  G  N  K  Y  E  Y  D  P  D  L  G  A  I

 121 AAGCTGGACCGGGTCCTGCCGGGAGCCCAGTTCTACCCCGGGGACTACGGCTTCATCCCC
  41 K  L  D  R  V  L  P  G  A  Q  F  Y  P  G  D  Y  G  F  I  P

 181 TCCACCCTGGCCGAGGACGGGGACCCCTTGGACGGCCTCGTCCTCTCCACCTACCCCCTC
  61 S  T  L  A  E  D  G  D  P  L  D  G  L  V  L  S  T  Y  P  L

 241 CTCCCCGGGGTGGTGGTGGAGGTCCGGGTGGTGGGCCTCCTCCTCATGGAGGACGAGAAG
  81 L  P  G  V  V  V  E  V  R  V  V  G  L  L  L  M  E  D  E  K

 301 GGCGGGGATGCCAAGGTCATCGGGGTGGTGGCCGAGGACCAGCGCCTGGACCACATCCAG
 101 G  G  D  A  K  V  I  G  V  V  A  E  D  Q  R  L  D  H  I  Q

 361 GACATCGGGGACGTCCCCGAGGGCGTGAAGCAAGAGATCCAGCACTTCTTTGAGACCTAC
 121 D  I  G  D  V  P  E  G  V  K  Q  E  I  Q  H  F  F  E  T  Y

 421 AAGGCCCTCGAGGCCAAGAAGGGGAAGTGGGTCAAGGTCACGGGCTGGCGGGACCGGAAG
 141 K  A  L  E  A  K  K  G  K  W  V  K  V  T  G  W  R  D  R  K

 481 GCGGCCTTGGAGGAGGTCCGGGCCTGCATCGCCCGCTACAAGGGCTAGGGGCTGAAAGGC
 161 A  A  L  E  E  V  R  A  C  I  A  R  Y  K  G  ***

 541 GCTTTCCGGGCCGGGGACGCCCCGGCCATTAGAATTCAGGGGGGTGTGCATGGTCTGCCC

 601 GGTCTGCGCGAGGCGCTGGAGCTGGAAGGGTACGAGGTGGGGGACCTCGTGGACTGCGAG

 661 GCCTGCGGGGCGGTCCTCCGCTCCTCTCTCCGATGGGGGCCTGGAGGTGGTGGTGCCCCG

 721 GGGGGGGAGAAGGAGCCTCTGGGGCCT
```

Fig. 2. **The nucleotide sequence of the gene and its deduced amino acid sequence for the inorganic pyrophosphatase from *Tth* HB8.** The nucleotides are numbered starting at the initiation codon, ATG (corresponding to a Met residue). The boxed and underlined nucleotides represent the −35 and −10 regions, respectively. Asterisks show the stop codon (TAG). The putative ribosome binding sequence and the deduced ρ-dependent terminator were indicated by lower-case letters and double underlining, respectively.

```
          1        10        20        30        40        50        60        70
          ANLKSLPVGDKAPEVVHMVIEVPRGSGNKYEYDPDLGAIKLDRVLPGAQFYPGDYGFIPSTLAEDGDPLD
intact    <-----------------/
V8        <------------>       <--------><--><-----><----------><---------><-----
API           <-----><---------------><---------><-----------------------------
Asp-Pro                                                                    <--

         71        80        90       100       110       120       130       140
          GLVLSTYPLLPGVVVEVRVVGLLLMEDEKGGDAKVIGVVAEDQRLDHIQDIGDVPEGVKQEIQHFFETYK
V8        ----><---------><--------> <-----------><-------><----><---><----><--
API       ----X----/                           <------------------------><--------->
Asp-Pro   ----------------------X---------/
BrCN                           <-----/

        141       150       160       170
          ALEAKKGKWVKVTGWRDRKAALEEVRACIARYKG
V8        --><-----------><-----><-------->
API       <---->   <-><------><------------>
```

Fig. 1. **The complete amino acid sequence of inorganic pyrophosphatase (PPase) from *Thermus thermophilus* (*Tth*) HB8.** The amino acid residues are shown as one-letter abbreviations. The arrows indicate the determined sequence for each peptide obtained on digestion with *S. aureus* V8 protease (V8) and *Achromobacter* protease I (API), and also on chemical cleavage with formate-pyridine (Asp-Pro) and cyanogen bromide (CNBr). The amino-terminal sequence was determined for the reduced and *S*-pyridylethylated enzyme (intact). X indicates a residues not identified.

9.0), followed by concentration to 1.5 mg·protein/ml. An aliquot of *Tth* PPase (0.5 mg) was digested with API (molar ratio, 1:100) at 37°C for 6 and 24 h. The reaction was stopped by adding 99% formate. The digested sample was centrifuged and filtered on a 0.45 μm membrane filter (Millipore), and then separated by reverse-phase HPLC on a Microsorb-MV column (RAININ) with a linear gradient of 0-80% acetonitrile in 0.1% TFA. The isolated peptides were sequenced by automatic Edman degradation using a PSQ-1 automatic gas-phase protein sequencer (Shimadzu).

Computer-Aided Protein Sequence Alignment—Alignment of the primary structures of several PPases was performed with the GENETYX program package (Software Development) on an Apple Macintosh Computer.

RESULTS

Determination of the Amino Acid Sequence of Tth PPase—The complete amino acid sequence of the PPase from *Tth* was determined by overlapping the sequences of

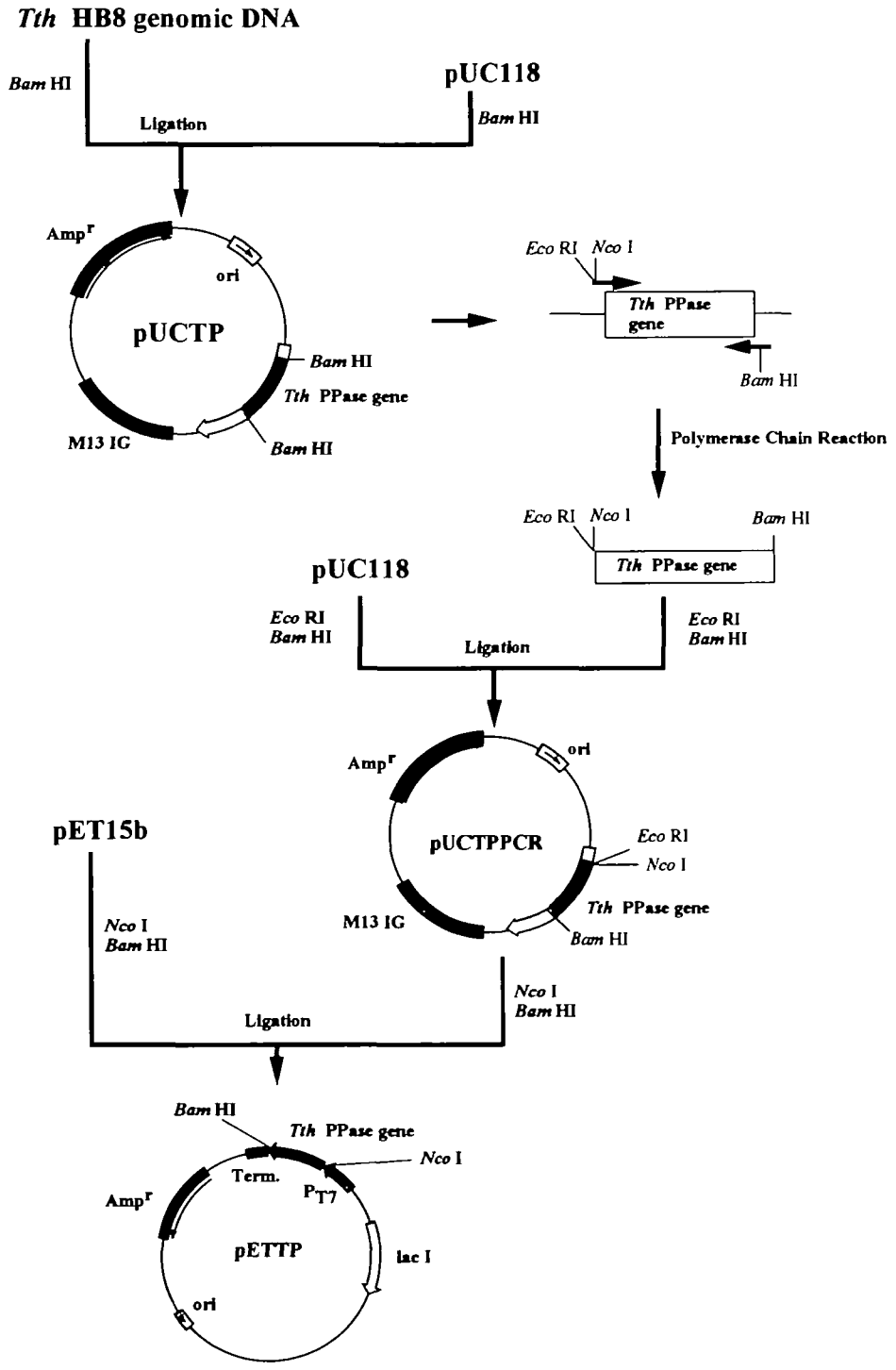

Fig. 3. **Construction of the cloning vector, pUCTP, and the expression vector, pETTP, for the *Tth* PPase gene.** A cloning vector for the *Tth* PPase gene, pUCTP, was constructed as described under "MATERIALS AND METHODS." The vector, pUCTP, was used as the template for PCR to construct pUCTPPCR, which contains introduced *Eco*RI, *Nco*I, and *Bam*HI sites. After digestion with *Nco*I and *Bam*HI, the *Tth* PPase gene fragment was inserted into the same site of the pET15b vector.

peptide fragments obtained on digestion with proteases and chemical cleavage after automatic Edman degradation. The sequence of the enzyme at the protein level was aligned based on the overlapping of at least two or more residues. Seventeen residues of the N-terminal region were sequenced by automatic Edman degradation of the entire *S*-pyridylethylated protein. And the C-terminal residue, Gly, was determined by treatment with carboxypeptidase P. Twenty-seven peptides were isolated from the V8 protease digest of the enzyme by reverse phase (RP)-HPLC, which were numbered in their order of elution and were almost all subjected to sequence analysis. The C-terminal residue of these digested fragments was either Glu or Asp, except for the (V8-19) fragment (residues 65-75), which ended with Ser, which may be due to non-specific cleavage by the V8 protease. But we could not detect residues 15-21 and 97-98. The alignment of the V8 protease fragments was mostly performed by sequencing of the isolated 19 peptides of the enzyme digested with API. We could not detect fragments corresponding to residues 1-4 and 146-148, and residue 81-104 could not be further sequenced to the C-terminal residue. The chemical cleavage of Asp-Pro by formic acid yielded 4 peptide fragments, which were separated by RP-HPLC, and only the third fragment (Asp-Pro) was sequenced. This peptide was only sequenced from residue 68 to 115, since it was too long for complete sequence analysis, and this sequencing was good enough to align and determine the whole sequence. Chemical cleavage with cyanogen bromide (BrCN) yielded four peaks, and only the second eluted fraction on RP-HPLC (BrCN-2, 96-174) was sequenced to 6 cycles. As a result, the complete amino acid sequence of *Tth* PPase was determined as shown in Fig. 1, 174 residues comprising the monomer chain of this enzyme.

Genomic Cloning and Base Sequence of Tth PPase—On the basis of the amino acid sequence determined above, we attempted to clone the *Tth* PPase gene to determine the thermostability of *Tth* PPase from the genetic information. At first, we prepared genomic DNA from *Tth* as described under "MATERIALS AND METHODS," which was digested with *Bam*HI. The mixture was explored by means of Southern hybridization at 68°C with a probe corresponding to nucleotide 85 to 416. As a result, it gave a single positive band corresponding to about 1.8 kbp, and the genomic *Bam*HI fragments were inserted into the multicloning site (MCS) of a plasmid vector, pUC118. Then, the colony hybridization of transformed *E. coli* JM109 was performed, which revealed only one positive colony among 50 colonies. The plasmid derived from this colony was found to contain an about 1.8 kbp fragment derived from genomic DNA, which included the open reading frame (ORF) coding for the putative sequence of the *Tth* PPase gene. This fragment was subcloned and sequenced in both directions after its digestion with several restriction enzymes. Its whole base sequence and the deduced amino acid sequence are shown in Fig. 2. The amino acid sequence deduced from the base sequence of this cloned gene coincided completely with the primary structure determined at the protein level. Also, we observed similar sequences to the −35 and −10 regions of the promoter upstream of the coding region of *Tth* PPase. Furthermore, downstream of the *Tth* PPase gene, a putative terminator region was present. Then, we confirmed that the structural gene of *Tth* PPase was cloned completely.

Expression of the Tth PPase Gene in E. coli BL21 (DE3)—As described above, cloning of the *Tth* PPase gene was accomplished. Therefore, we tried to establish an expression system for *Tth* PPase in *E. coli*. The cloning vector of the *Tth* PPase gene, pUCTP, was used as the template for PCR in order to construct an expression vector. As described under "MATERIALS AND METHODS," the DNA fragment amplified by PCR was inserted into the *Eco*RI-*Bam*HI site of a plasmid vector, pUC118 (pUCTPP-CR) and then sequenced. Using this pUCTPPCR plasmid, the pETTP vector for expression in *E. coli* BL21(DE3) was constructed as shown in Fig. 3. After digestion of pUCTPP-CR with *Nco*I and *Bam*HI endonucleases, the resultant fragment was inserted into the *Nco*I-*Bam*HI site of the pET15b vector. Then, *E. coli* cells were transformed with the expression vector, and cultured in LB/Amp medium. The cell extract was examined by SDS-PAGE, and expression of the *Tth* PPase was confirmed in the extract of *E. coli* BL21(DE3)/pETTP. Starting with 6 g wet cells per 1 liter

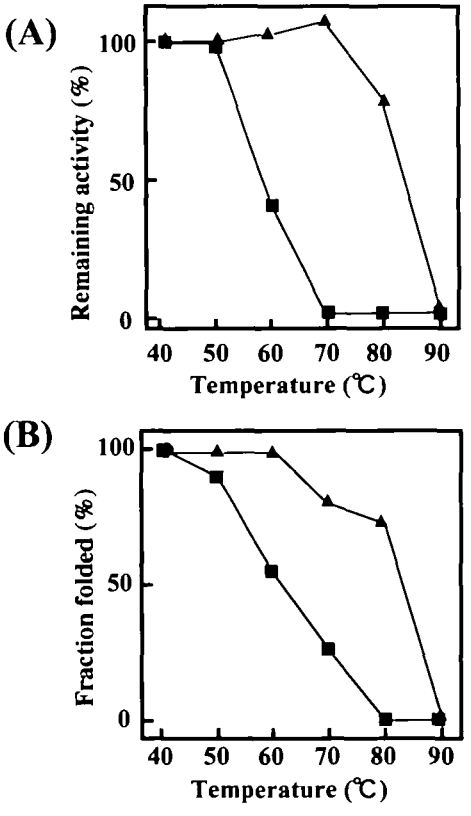

Fig. 4. **Thermostability of the recombinant *Tth* and *E. coli* PPases.** Each enzyme solution (0.1 mg/ml) was incubated in Tris-HCl buffer (pH 7.8) at the indicated temperature for 1 h. (A) The remaining activities of the two enzymes after heat incubation. The enzyme activity was measured at 37°C. The activity after incubation at 40°C was taken as 100%. (B) Conformational changes of the both enzymes after heat incubation, as detected with CD spectra. The relative ellipticity of the CD band at 222 nm is plotted against the temperature taking the value at 40°C as 100% and that at 90°C as 0%. The ratio was calculated with the following equation. Fraction folded (ratio of native protein) = $(Y - Y_D) \times 100/(Y_N - Y_D)$, where Y_D and Y_N are the mean residue ellipticities, $[\theta]$, at 222 nm after incubation at 90 and 40°C, respectively, and Y is the measured mean residue ellipticity at the indicated temperature. Symbols: (■) recombinant *E. coli* PPase; (▲) recombinant *Tth* PPase.

culture, the recombinant *Tth* PPase was purified to an electrophoretically homogeneous state, as described under "MATERIALS AND METHODS." The yield of the purified enzyme was about 10 mg, and the specific activity was 200-500 units/mg when the activity was measured at 37°C.

Characterization of the Recombinant Tth PPase—The recombinant *Tth* PPase was obtained effectively, therefore, we examined some of its characteristics. The sequence of the N-terminal 12 residues was the same as that in Fig. 1, without the initiation Met residue being detected. The results of amino acid composition analysis of the recombinant enzyme were almost identical with those for the authentic enzyme. The secondary structure of the recombinant enzyme was examined by measuring the CD spectrum in the far-UV region. This spectrum indicated that the recombinant enzyme contains abundant α-helices and β-forms, and its profile resembled that of *E. coli* PPase (data not shown). Meanwhile, the thermostability of the recombinant enzyme was measured in 20 mM Tris-HCl buffer (pH 7.8). As shown in Fig. 4A, the recombinant *Tth* enzyme was highly thermostable, it not being inactivated completely on incubation at 90°C, whereas the *E. coli* enzyme was inactivated completely at 70°C. Furthermore, to obtain information on the change in the secondary structure on heating, it was chased with far-UV CD spectra as the criterion. The spectra of the recombinant *Tth* enzyme did not change on heating up to 80°C, which suggested that the secondary structure was retained even at 80°C, as shown in Fig. 4B. Therefore, these results showed that the recombinant *Tth* PPase must be endowed with the same thermostability as the authentic enzyme (*25*).

Limited Proteolysis of the Recombinant Tth PPase by Digestion with API—As described above, the recombinant *Tth* PPase exhibited the same characteristics as the authentic enzyme. Then, we investigated the conformation of the recombinant *Tth* PPase in solution by limited proteolysis to determine whether or not the recombinant enzyme differs in conformation from the authentic enzyme as reported previously (*10*). Based on the information on the three-dimensional structure of the authentic *Tth* PPase (*10*), we selected *Acromobacter* protease I (API) from among many proteases. Because several Lys residues are present in the active-site pocket, and the hydrophilicity of a Lys residue enhances the probability of its presence on the surface of a molecule, it was expected that the *Tth* enzyme was cleaved on the C-terminal side of some Lys residues on the surface by API. When the recombinant enzyme was digested with API for 6 h, 23 peptide fragments were separated on reverse phase HPLC, although there must be 15 peptides theoretically, while 34 peptides were detected after 24 h. The digestion fragments after 6 and 24 h were sequenced

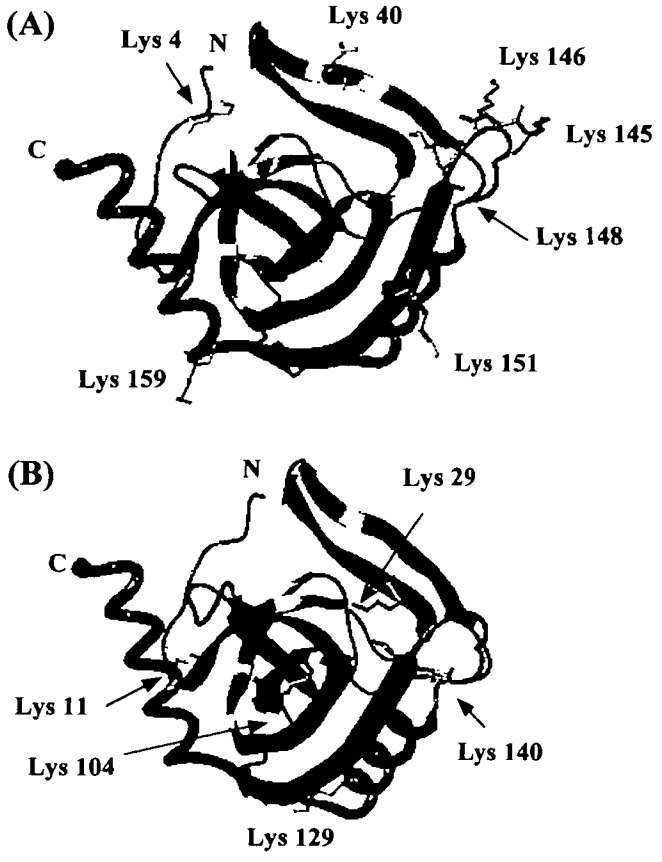

Fig. 5. **Cleavage sites in the three-dimensional structure (ribbon representation) of the *Tth* PPase subunit on digestion with API.** (A) Cleavage sites on digestion for 6 h. (B) Cleavage sites on digestion for 24 h. N and C indicate the amino- and carboxy-termini, respectively.

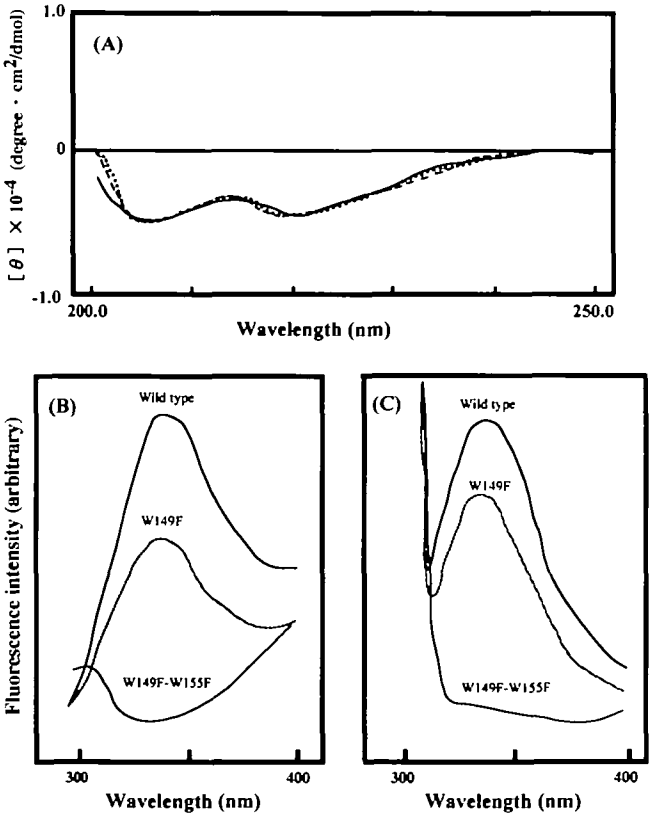

Fig. 6. **CD and fluorescence spectra of the recombinant *Tth* PPase (wild type) and its variants, W149F and W149F-W155F.** (A) CD spectra in the far-UV region. (—) wild type; (- - -) W149F; (·····) W149F-W155F. (B) Fluorescence emission spectra with excitation at 275 nm. (C) Fluorescence emission spectra with excitation at 295 nm. The protein concentration was 0.1 mg/ml in 20 mM Tris-HCl buffer (pH 7.8).

by automatic Edman degradation. In the case of digestion for 6 h, the C-terminal sides of the Lys4, Lys40, Lys145, Lys146, Lys148, Lys151, and Lys159 residues were cleaved. Furthermore, the additional cleavage on Lys11, Lys29, Lys104, Lys129, and Lys140 was confirmed after 24 h. Figure 5, A and B, show the cleavage sites in a model of the *Tth* PPase molecule on digestion with API for 6 and 24 h, respectively. The environment of Lys residues in the recombinant *Tth* PPase may be similar to that in the authentic enzyme.

Substitution of Tryptophan Residues in the Tth PPase by Site-Directed Mutagenesis and Its Effect on Thermostability—From the results of studies on chemical modification, some candidate amino acids taking part in the catalysis and stability of the molecule have been deduced. Trp149 of two Trp residues in *E. coli* PPase affects Mg^{2+} binding (*26*). In the case of Y-PPase (*27*) and PS-3 PPase (*28*), Trp residues were also very effective as to Mg^{2+}-binding. Therefore, we expected that either of the two Trp residues in the *Tth* PPase may be related with the Mg^{2+} binding and Mg^{2+}-induced thermostability directly. Therefore, in order to increase our understanding of the role of the Trp residues in PPase, we examined the relationship between the Trp residues and the thermostability or Mg^{2+}-induced thermostability by site-directed mutagenesis. Two Trp-substituted variants, W149F and W149F-W155F, were constructed as described under "MATERIALS AND METHODS." The specific activities of the two variants were 151 and 53 units/mg, respectively, while that of the wild type was 222 units/mg under the standard conditions. To explain the significant reduction in the specific activities of the two variants, their CD spectra in the far-UV region and fluorescence spectra were measured, as shown in Fig. 6. Their CD spectra were almost identical with that of the wild type, while complete quenching of the fluorescence spectrum for W149F-W155F was observed. On the other hand, the W149F variant showed appreciable quenching. These results suggested that the secondary structure could be maintained even if either or both Trp residues were replaced by Phe in the *Tth* PPase, and the environment around Trp155 was not affected by the absence of Trp149. Furthermore, the thermostabilities of the two variants after heating for 1 h were measured as their activity, CD and fluorescence spectra, as shown in Fig. 7. Without the addition of Mg^{2+}, the two Trp variants showed lower thermostabilities than that of the wild type in terms of activity and fluorescence spectra, as shown in Fig. 7, A and C. However, the behavior as to Mg^{2+}-induced thermostability was somewhat different between the wild type and the two variants. W149F showed almost the same degree of thermostability as the wild type in the presence of 1 mM Mg^{2+} (Fig. 7, B and D). On the other hand, W149F-W155F showed no change in the activity even in the presence of Mg^{2+} (Fig. 7B). This suggested that Trp155 might be responsible for the Mg^{2+}-induced thermostabilization of the *Tth* PPase, whereas Trp149 may contribute to the thermostability of the *Tth* PPase itself. From this viewpoint, we need to determine the kinetic parameters, in

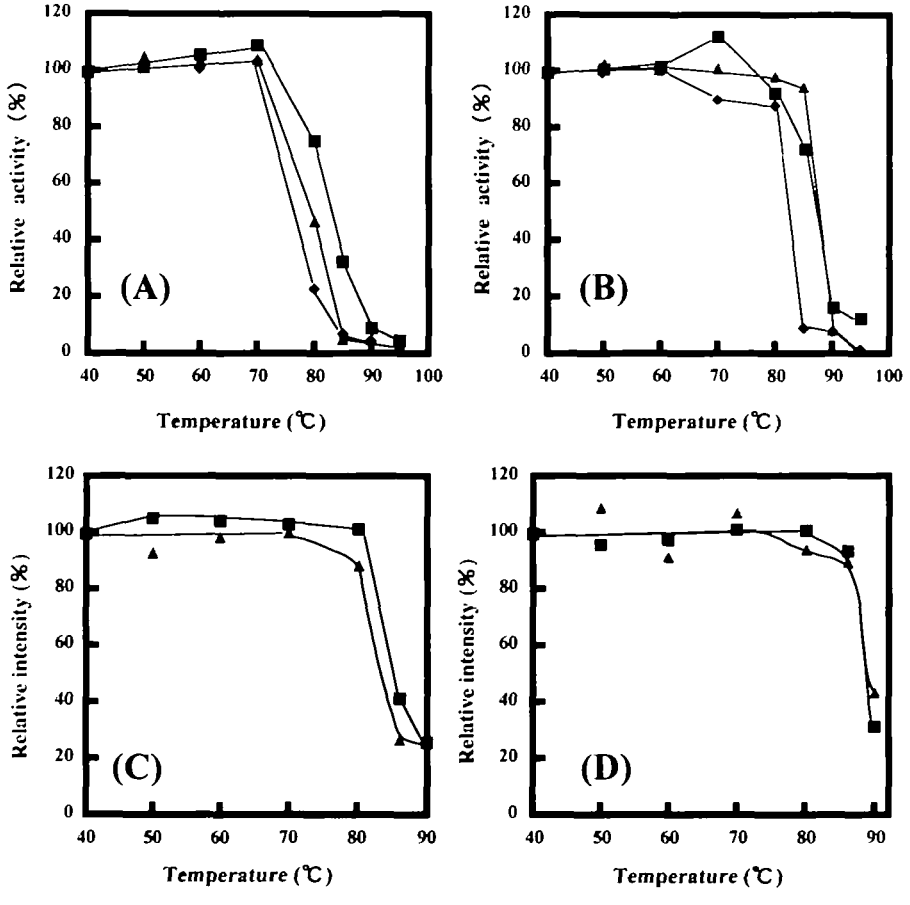

Fig. 7. **Thermal stability of the recombinant *Tth* PPase (wild type) and its variants, W149F and W149F-W155F.** The remaining activity of each enzyme was measured at 37°C after heat incubation for 1 h. The activity after incubation at 40°C was taken as 100%. (A) No Mg^{2+} addition; (B) in the presence of 1 mM Mg^{2+}. On the other hand, the fluorescence spectra were measured under the following conditions; each enzyme was incubated in 20 mM Tris-HCl buffer (pH 7.8) at the indicated temperature for 1 h. After heating, the emission spectrum of each sample was measured with excitation at 295 nm. The fluorescence intensity at the maximum wavelength was plotted as the relative value to that at 40°C. (C) No Mg^{2+} addition; (D) in the presence of 1 mM Mg^{2+}. Symbols: (■) wild type; (▲) W149F; (◆) W149F-W155F.

general, of the variants as to Mg^{2+}-binding, and some characterization is now underway.

DISCUSSION

The inorganic pyrophosphatase from *Tth* HB8 was very thermostable, and further heat stabilization was induced by Mg^{2+}, as reported previously (*25*). It has been suggested that several procaryotic PPases are also able to become thermostable through binding with divalent cations such as Mg^{2+}. In view of these two types of thermostability, *i.e.* intrinsic and Mg^{2+}-induced ones, we tried to solve this problem by amino acid or base sequence comparison, employing limited proteolysis and site-directed mutagenesis.

At first, the primary structure of PPase from *Tth* HB8 (authentic *Tth* PPase) was determined directly at the protein level and then by deduction from its base sequence. Although we have already presented some information on the amino acid sequence for determining the three-dimensional structure of this enzyme (*10*), we strictly confirmed that the determined amino acid sequence coincided with that deduced from its base sequence. At the protein level, we have determined the complete amino acid sequence of the authentic *Tth* PPase by Edman degradation (Fig. 1). Genomic cloning of the *Tth* PPase was completed, as described above, and consequently the base sequence and its deduced amino acid sequence could be determined (Fig. 2). The amino acid sequence deduced from the gene coincided well with the sequence determined at the protein level. From this information, we determined that the *Tth* PPase consists of 174 amino acid residues per monomer with a calculated molecular weight of 19,072. The alignment of the amino acid sequences of several PPases and the *Tth* PPase is shown in Fig. 8, and the relative homology between several PPases is shown in Table I. Teplyakov *et al.* reported the three-dimensional structure of this enzyme (*10*), which indicated that the conserved 15 residues (Glu21, Lys29, Glu31, Arg43, Tyr51, Tyr55, Asp65, Asp67, Asp70, Asp97, Asp102, Lys104, Tyr139, Lys140, and Lys148) reside in the active-site cavity of the *Tth* PPase. Our information on the primary structure of the *Tth* PPase will reinforce and confirm this identification of the active center of this enzyme.

On the other hand, genetic information on the *Tth* PPase was obtained by molecular cloning of its gene. As described above, it contained the structural gene of the *Tth* PPase, which corresponds to the promoter region, initiation codon, open reading frame (522 bp), stop codon, and terminator region. In the structural gene, the promoter region was deduced from the homology between the *E. coli* PPase gene and the cloned *Tth* PPase gene. We found that the −35 region was 5′-TGGCCC-3′, whereas the −10 region was CATAAT, and the interval between the two regions was 19 bp. To confirm that this promoter from *Tth* acts in *E. coli* cells functionally, a cloned plasmid, pUCTP, was transformed into *E. coli* JM109, which was then cultured. The cell extract was analyzed by SDS-PAGE so that we could estimate that the *Tth* PPase was expressed in *E. coli* cells by utilizing the promoter from *Tth* HB8. Furthermore, we deduced a ribosome binding sequence from the homology between various genes of *Tth* HB8 (*29-32*), and from the sequence of *Tth* HB8 16s rRNA (*33*). The putative sequence was GGCGG at nucleotides −6 to −2 (Fig. 2). The initiation codon of the *Tth* PPase gene was ATG, however, the corresponding Met residue would be eliminated on translation, as described above. On the other hand, the stop codon was TAG in the *Tth* PPase gene, whereas the *E. coli* PPase gene it was TAA. Furthermore, deduction of the terminator region was performed with the GENETYX program (Software Development). In the case of the *E. coli* PPase gene, the terminator region was 20 bp downstream of the stop codon (*7*). The putative terminator of the *Tth* PPase gene exists about 90 bp downstream from the stop

TABLE I. **Relative homology of amino acid sequences of several inorganic PPases from eucaryotic and procaryotic bacteria (%).**

	S.ce	*K.la*	*S.po*	*A.th*	*T.ac*	*E.co*	PS-3
K.la	84.6						
S.po	70.1	71.6					
A.th	22.2	21.6	22.6				
T.ac	30.3	30.7	27.2	44.9			
E.co	31.2	33.8	25.0	37.1	42.4		
PS-3	26.3	30.9	30.0	40.4	44.2	46.4	
Tth	24.8	27.4	30.2	40.1	43.5	47.4	48.4

S.ce, Saccharomyces cerevisiae (Ref. *6*). *K.la, Kluyveromyces lactis* (Ref. *35*). *S.po, Schizosaccharomyces pombe* (Ref. *36*). *A.th, Arabidopsis thaliana* (Ref. *37*). *T.ac, Thermoplasma acidophilum* (Ref. *34*). *E.co, Escherichia coli* (Ref. *7*). PS-3, thermophilic bacterium PS-3 (Ref. *9*).

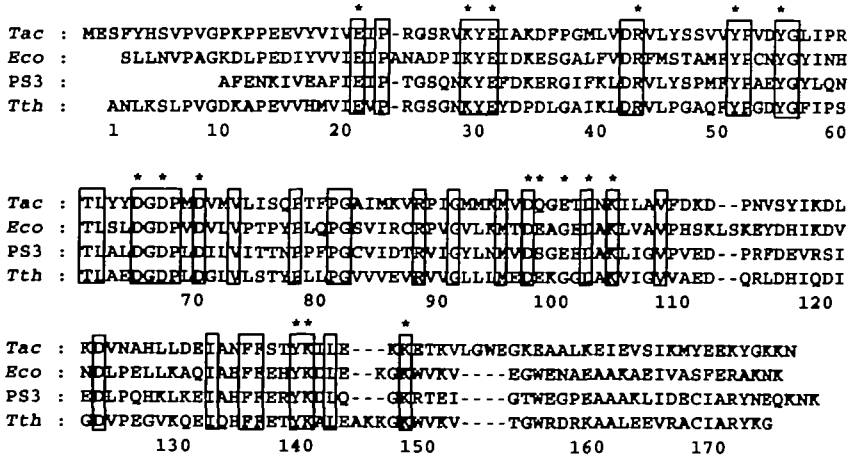

Fig. 8. **Alignment of the amino acid sequences of various PPases.** The amino acid sequences of PPases from *T. acidophilum* (*Tac*), *E. coli* (*Eco*), and thermophilic bacterium PS-3 (*PS3*) were aligned using the computer program, GENETYX. Asterisks indicate the putative active site residues based on the tertiary structure of *Tth* PPase (*10*). The boxed amino acids represent invariant residues among all the PPases. The numbering of the residues is that of *Tth* PPase.

codon, which formed 12 hydrogen-bonds in a hairpin structure, and the most stabilized form as to energy (Fig. 2). It is considered that this terminator is a type of ρ-dependent terminator, the same as reported for *Thermoplasma acidophilum* PPase (*34*). Overall, the G and C base content in the *Tth* PPase gene (67.4%) was higher than those of several cloned bacterial PPase genes. The G and C base would be favored for the third letter in codon usage, whose content was 96.6%, while that of the *E. coli* PPase gene was 59.3%. At the DNA level, it seemed likely that the *Tth* PPase gene must also adopt the G and C base for thermostabilization as much as possible.

Furthermore, we have established an expression system for the *Tth* PPase in *E. coli* cells. As described above, an expression vector, pETTP, for the *Tth* PPase was constructed and effectively expressed in *E. coli* BL21(DE3) cells (Fig. 3). The estimated molecular weight of the expressed product was about 19 kDa, which exhibits good agreement with that calculated from the determined amino acid sequence. After purification to an electrophoretically homogenous state, the characteristics of the product were analyzed. Its N-terminal 12 residues and amino acid composition were identical with those of the authentic enzyme. And some characteristics of the product, such as enzyme activity, secondary structure, and thermostability, implied that the expressed product must be the same that of the authentic *Tth* PPase reported previously (*25*). Thus, we have succeeded in expression of the recombinant *Tth* PPase in *E. coli* cells.

The next step in investigating the thermostability of the *Tth* PPase was to elucidate the structure of the recombinant enzyme in solution. As described above, the three-dimensional structure of the authentic *Tth* PPase had been determined by X-ray diffraction at 2.0 Å (*10*). On the basis of this conformational information, we have compared the results on limited proteolysis with this information (Fig. 5). When the enzyme was digested with API for 6 h, it was cleaved on the C-terminal sides of Lys4, Lys40, Lys145, Lys146, Lys148, Lys151, and Lys159. The results indicated that these lysine residues must be localized on the surface of the recombinant *Tth* PPase molecule. Salminen *et al.* reported that Lys40 could form intratrimeric hydrophilic contacts with Glu86, while Lys145 may form intertrimeric hydrophilic contacts with Gln130 (*14*). It is also expected from the deduced B-factor that these Lys residues are present in a hydrophilic environment. Furthermore, it was apparent from the results of API digestion for 24 h that cleavage also occurred on the C-terminal sides of Lys11, Lys29, Lys104, Lys129, and Lys140. In particular, Lys29 and Lys104 would be present in the active center of the *Tth* PPase, and some interactions occurred around these residues. Because of these interactions, these five Lys residues were more resistant to proteolysis than the other residues described above. These results indicated that Lys29 and Lys104 may be located in a more interior region of the molecule than Lys140 in the active-site cavity. From the results of the study involving limited proteolysis, we can conclude that the environment of Lys residues in the recombinant *Tth* PPase in solution may be very similar to that in the crystal state.

Finally, we investigated the relationship between Trp residues and thermostability by site-directed mutagenesis. The *Tth* PPase has two Trp residues, therefore, two Trp-substituted variants, W149F and W149F-W155F, could be constructed as described under "MATERIALS AND METHODS." The specific activities of these variants were appreciably reduced, but their secondary structures showed almost no change, as indicated by far-UV CD spectra (Fig. 6A). However, the fluorescence spectrum of W149F with excitation at 295 nm showed slight quenching, but its emission maximum was not affected (Fig. 6, B and C). This quenching may be caused by the removal of Trp149, and the spectrum reflected the environmental state in the vicinity of the remaining Trp155. From these results, we can assume that the environment around Trp155 may not be affected by the removal of Trp149, because we could not detect any shift of the maximum. And the thermostabilities of the recombinant wild-type, W149F and W149F-W155F were examined as their activity, far-UV CD spectra, and fluorescence spectra. The results indicated that the two variants became more unstable, to the same extent, than the wild type in both activity and conformation. Thus, we suggested that Trp149 may be responsible for the thermostability of the *Tth* PPase. We also found that the wild type enzyme suffered an effect called "heat activation" between 65 and 80°C in the presence and absence of 1 mM Mg^{2+}. On the contrary, the thermostabilities of the two variants were not affected on heat activation (Fig. 7A). Meanwhile, W149F and the wild type exhibited appreciable Mg^{2+}-induced thermostability, but W149F-W155F was little affected on the addition of Mg^{2+} (Fig. 7B). We suggest that Trp155 may somehow contribute to the Mg^{2+}-induced thermostability of the *Tth* PPase because we detected a very weak or no effect on Mg^{2+} addition in the case of the W149F-W155F variant. The three-dimensional structure of the *Tth* PPase demonstrated that the two Trp residues are present in the vicinity of the active-site cavity. However, we have never obtained the evidence that the Trp residues could bind to the substrate and Mg^{2+} directly. We can explain these results and the role of the Trp residues in thermostability as follows; we can predict that Trp149 exists in a flexible region, referred to the B-factor, from the data on X-ray crystallography, and that intersubunit hydrogen-bonding occurs between Trp149 and Glu98, as reported previously (*10*). It was deduced that Trp149 may affect the thermostability of the molecule itself due to the effect of this interaction and flexibility, which would be responsible for the structural integrity. On the other hand, Trp155 is present in the internal β-sheet, and the flexibility around this residue would be very small, as expected for the B-factor, and the hydrogen-bonding was not confirmed for this residue. These results indicated that Trp155 exists in the neighborhood of the active-site cavity and affects the Mg^{2+}-induced thermostability. However, from the information on the three-dimensional structure, we suggest that Trp155 can not bind with Mg^{2+} and the substrate. Thus, we postulate that the role of Trp155 may be as an indirect regulator of the Mg^{2+} binding. Although we need to perform further detailed investigations, we can conclude that the two Trp residues in the *Tth* PPase must be related to the two types of thermostability, that is the intrinsic and Mg^{2+}-induced ones.

We wish to thank M. Yashima, H. Kan, and S. Kawata for their contributions in the purification, characterization, and limited proteolysis. Our thanks are also due to N. Sakurai, K. Shibuya, T.

Sasaki, T. Wakabayashi, and H. Shinoda for the fruitful discussions.

REFERENCES

1. Josse, J. and Wong, S.C.K. (1971) Inorganic pyrophosphatase of *Escherichia coli* in *The Enzymes* (Boyer, P.D., ed.) 3rd. Vol. 4, pp. 499-527, Academic Press, New York
2. Cooperman, B.S., Baykov, A.A., and Lahti, R. (1992) Evolutionary conservation of the active site of soluble inorganic pyrophosphatase. *Trends Biochem. Sci.* **17**, 262-266
3. Salminen, T., Käpylä, J., Heikinheimo, P., Kankare, J., Goldman, A., Heinonen, J., Baykov, A.A., Cooperman, B.S., and Lahti, R. (1995) Structure and function analysis of *Escherichia coli* inorganic pyrophosphatase: Is a hydroxide ion the key to catalysis? *Biochemistry* **34**, 782-791
4. Baykov, A.A., Hyytia, T., Volk, S.E., Kasho, V.N., Vener, A.V., Goldman, A., Lahti, R., and Cooperman, B.S. (1996) Catalysis by *Escherichia coli* inorganic pyrophosphatase: pH and Mg^{2+} dependence. *Biochemistry* **35**, 4655-4661
5. Heikinheimo, P., Pohjanjoki, P., Helminen, A., Tasane, M., Cooperman, B.S., Goldman, A., Baykov, A.A., and Lahti, R. (1996) A site-directed mutagenesis study of *Saccharomyces cerevisiae* pyrophosphatase. Functional conservation of the active site of soluble inorganic pyrophosphatase. *Eur. J. Biochem.* **239**, 138-143
6. Kolakowski, L.F., Schlösser, M., and Cooperman, B.S. (1988) Cloning, molecular characterization and chromosome localization of the inorganic pyrophosphatase (PPA) gene from *S. cerevisiae*. *Nucleic Acids Res.* **22**, 10441-10452
7. Lahti, R., Pitkäranta, T., Valve, E., Ilta, I., Kukko-Kalske, E., and Heinonen, J. (1988) Cloning and characterization of the gene encoding inorganic pyrophosphatase of *Escherichia coli* K-12. *J. Bacteriol.* **170**, 5901-5907
8. Ichiba, T., Takenaka, O., Samejima, T., and Hachimori, A. (1990) Primary structure of the inorganic pyrophosphatase from thermophilic bacterium PS-3. *J. Biochem.* **108**, 572-578
9. Maruyama, S., Maeshima, M., Nishimura, M., Aoki, M., Ichiba, T., Sekiguchi, J., and Hachimori, A. (1996) Cloning and expression of the inorganic pyrophosphatase gene from thermophilic bacterium PS-3. *Biochem. Mol. Biol. Int.* **40**, 679-688
10. Teplyakov, A., Obmoloba, G., Wilson, K.S., Ishii, K., Kaji, H., Samejima, T., and Kuranova, I. (1994) Crystal structure of inorganic pyrophosphatase from *Thermus thermophilus*. *Protein Sci.* **3**, 1098-1107
11. Harutyunyan, E.H., Oganessyan, V.Y., Oganessyan, N.N., Avaeva, S.M., Nazarova, T.I., Vorobyeva, N.N., Kurilova, S.A., Huber, R., and Mather, T. (1997) Crystal structure of holo inorganic pyrophosphatase from *Escherichia coli* at 1.9 Å resolution. Mechanism of hydrolysis. *Biochemistry* **36**, 7754-7760
12. Kankare, J., Salminen, T., Lahti, R., Cooperman, B.S., Baykov, A.A., and Goldman, A. (1996) Crystallographic identification of metal-binding sites in *Escherichia coli* inorganic pyrophosphatase. *Biochemistry* **35**, 4670-4677
13. Heikinheimo, P., Lehtonen, J., Baykov, A.A., Lahti, R., Cooperman, B.S., and Goldman, A. (1996) The structural basis for pyrophosphatase catalysis. *Structure* **4**, 1491-1508
14. Salminen, T., Teplyakov, A., Kankare, J., Cooperman, B.S., Lahti, R., and Goldman, A. (1996) An unusual route to thermostability disclosed by the comparison of *Thermus thermophilus* and *Escherichia coli* inorganic pyrophosphatases. *Protein Sci.* **5**, 1014-1025
15. Obmolova, G., Kuranova, I., and Teplyakov, A. (1993) Purification, crystallization and preliminary X-ray analysis of inorganic pyrophosphatase from *Thermus thermophilus*. *J. Mol. Biol.* **232**, 312-313
16. Friedman, M., Krull, L.H., and Cavins, J.F. (1970) The chromatographic determination of cystine and cysteine residues in protein as s-beta-(4-pyridylethyl) cysteine. *J. Biol. Chem.* **245**, 3868-3871
17. Chung, C.T., Niemela, S.L., and Miller, R.H. (1989) One-step preparation of competent *Escherichia coli*: transformation and storage of bacterial cells in the same solution. *Proc. Natl. Acad. Sci. USA* **86**, 2172-2175
18. Yoshizaki, F., Oshima, T., and Imahori, K. (1971) Studies on phosphoglucomutase from an extreme thermophile, *Flavobacterium thermophilum* HB8. I. Thermostability and other enzymatic properties. *J. Biochem.* **69**, 1083-1089
19. Maniatis, T., Fritsh, E.F., and Sambrook, F.J. (1982) *Molecular Cloning: A Laboratory Manual*, pp. 196, Cold Spring Harbor Laboratory, Cold Spring Habor, New York
20. Innis, M.A., Gelfand, D.H., Sninsky, J.J., and White, T.J. (1990) *PCR Protocols. A Guide to Methods and Applications*, Academic Press, San Diego
21. Hachimori, A., Takeda, A., Kaibuchi, M., Ohkawara, N., and Samejima, T. (1975) Purification and characterization of inorganic pyrophosphatase from *Bacillus stearothermophilus*. *J. Biochem.* **77**, 1177-1183
22. Peel, J.H. and Loughman, B.C. (1957) Some observations on the role of copper ions in the reduction of phosphomolybdate by ascorbic acid and their application in the determination of inorganic pyrophosphate. *Biochem. J.* **65**, 709-716
23. Lowry, O.H., Rosebrough, N.J., Farr, A.L., and Randall, R.J. (1951) Protein measurement with the Folin phenol reagent. *J. Mol. Chem.* **193**, 265-275
24. Laemmli, U.K. (1970) Cleavage of structural proteins during the assembly of the head of bacteriophage T4. *Nature* **227**, 680-685
25. Höhne, W.E., Wessner, H., Kuranova, I.P., and Obmolova, G.V. (1988) Kinetics characterization of a thermostable inorganic pyrophosphatase from *Thermus thermophilus*. *Biomed. Biochim. Acta* **47**, 941-947
26. Kaneko, S., Ichiba, T., Hirano, N., and Hachimori, A. (1993) Modification of tryptophan 149 of inorganic pyrophosphatase from *Escherichia coli*. *Int. J. Biochem.* **25**, 233-238
27. Negi, T., Samejima, T., and Irie, M. (1972) Studies on the tryptophan residues of yeast inorganic pyrophosphatase in relation to the enzymatic activity. *J. Biochem.* **71**, 29-37
28. Kaneko, S., Ichiba, T., Hirano, N., and Hachimori, A. (1991) Modification of a single tryptophan of the inorganic pyrophosphatase from thermophilic bacterium PS-3: possible involvement in its substrate binding. *Biochim. Biophys. Acta* **1077**, 281-284
29. Xu, J., Seki, M., Denda, K., and Yoshida, M. (1991) Molecular cloning of phosphofructokinase 1 gene from a thermophilic bacterium, *Thermus thermophilus*. *Biochem. Biophys. Res. Commun.* **176**, 1313-1318
30. Kato, R. and Kuramitsu, S. (1993) RecA protein from an extremely thermophilic bacterium, *Thermus thermophilus* HB8. *J. Biochem.* **114**, 926-929
31. Motohashi, K., Yohda, M., Endo, I., and Yoshida, M. (1996) A novel factor required for the assembly of the DnaK and DnaJ chaperones of *Thermus thermophilus*. *J. Biol. Chem.* **271**, 17343-17348
32. Amada, K., Yohda, M., Odaka, M., Endo, I., Ishii, N., Taguchi, H., and Yoshida, M. (1995) Molecular cloning, expression, and characterization of chaperonin-60 and chaperonin-10 from a thermophilic bacterium, *Thermus thermophilus*. *J. Biochem.* **118**, 347-354
33. Hartmann, R.K. and Erdmann, V.A. (1989) *Thermus thermophilus* 16S rRNA is transcribed from an isolated transcription unit. *J. Bacteriol.* **171**, 2933-2941
34. Richter, O.M.H. and Schäfer, G. (1992) Cloning and sequencing of the gene for the cytoplasmic inorganic pyrophosphatase from the thermoacidophilic archaebacterium *Thermoplasma acidophilum*. *Eur. J. Biochem.* **209**, 351-355
35. Stark, M.R. and Milner, J.S. (1989) Cloning and analysis of the *Kluyveromyces lactis* TRP1 gene: a chromosomal locus flanked by genes encoding inorganic pyrophosphatase and histone H3. *Yeast* **5**, 35-50
36. Kawasaki, I., Adachi, N., and Ikeda, H. (1990) Nucleotide sequence of *S. pombe* inorganic pyrophosphatase. *Nucleic Acids Res.* **18**, 5888
37. Kieber, J.J. and Signer, E.R. (1991) Cloning and characterization of an inorganic pyrophosphatase gene from *Arabidopsis thaliana*. *Plant Mol. Biol.* **16**, 345-348